Biosensors and Bioelectronics 220 (2023) 114913

Contents lists available at ScienceDirect

Biosensors and Bioelectronics

journal homepage: www.elsevier.com/locate/bios

Combinatorial perturbation sequencing on single cells using microwell-based droplet random pairing

Run Xie [a,b,c,1], Yang Liu [c,1], Shiyu Wang [c], Xuyang Shi [c], Zhantao Zhao [a,b], Longqi Liu [c], Ya Liu [c,d,**], Zida Li [a,b,*]

[a] Department of Biomedical Engineering, Health Science Center, Shenzhen University, Shenzhen, 518060, China
[b] Guangdong Key Laboratory for Biomedical Measurements and Ultrasound Imaging, Department of Biomedical Engineering, Health Science Center, Shenzhen University, Shenzhen, 518060, China
[c] BGI-Shenzhen, Shenzhen, 518083, China
[d] Shenzhen Key Laboratory of Single-Cell Omics, BGI-Shenzhen, Shenzhen, 518100, China

ARTICLE INFO

Keywords:
Drug screening
Single-cell RNA sequencing
Droplet microfluidics
High throughput assay

ABSTRACT

Combinatorial drug therapy reduces drug resistance and disease relapse, but informed drug combinations are lacking due to the high scale of possible combinations and the relatively simple phenotyping strategies. Here we report combinatorial perturbation sequencing (CP-seq) on single cells using microwell-base droplet random pairing. CP-seq uses oligonucleotides to barcode drugs, encapsulates drugs and cells in separate droplets, and pairs cell droplets with two drug droplets randomly on a microwell array chip to complete combinatorial drug treatment and barcode-tagging on cells. The subsequent single-cell RNA sequencing simultaneously detects the single-cell transcriptomes and drug barcodes to demultiplex the corresponding drug treatment. The microfluidic droplet operations had robust performance, with the overall utilization rate of the microwells being up to 83%. We then progressively validated the CP-seq by performing single-drug treatments and then combinatorial-drug treatments, confirming the CP-seq's capability in the collection and analysis of drug-perturbed transcriptomes. Leveraging the advantage of droplet microfluidics in massive multiplexing, the CP-seq represents a great technology for combinatorial perturbation screening with high throughput and comprehensive profiling.

1. Introduction

Current drug discovery primarily aims to find agents that target a specific signaling pathway. However, due to the redundancy of cell signaling and the inter-cellular heterogeneity, using these drugs alone sometimes leads to suboptimal results. Relapse may arise due to previously unaware drug resistance existing in the cell population (Brown et al., 2014). Combinatorial drug therapy using multiple targets can potentially serve as a better treatment strategy (Al-Lazikani et al., 2012). By simultaneously targeting multiple mechanisms, combinatorial drug therapy can significantly reduce the chance of relapse (Jaaks et al., 2022). Indeed, the efficacy of this strategy has been demonstrated in treating bacterial infections with multiple antibiotics (León-Buitimea et al., 2020). In addition, a few combinatorial chemotherapies for cancer treatment have been approved by the Food and Drug Administration of the United States (Bhutani et al., 2021).

Nevertheless, drug combinations with informed efficacy are still limited. A major reason is the formidable workload in performing combinatorial screening. For example, the number of two-drug combinations in a library with 1,000 drugs is almost half a million, and the number of combinations of three or more drugs can be even more huge. Though the liquid handler-based (HTS) tools permit automated experiments with minimal human intervention, experiments with such high volume are still costly both time-wise and finance-wise (Zeng et al., 2020).

In addition, currently, the characterization of drug effects mainly relies on a few simple phenotypes, such as proliferation, morphology, and a handful of biomarkers. The limited biological insights on the drug effects can be inadequate to identify the mechanism of action and detect off-target effects, potentially leading to drug failures in preclinical or

* Corresponding author. Department of Biomedical Engineering, Health Science Center, Shenzhen University, ShenzhenShenzhen, 518060, China.
** Corresponding author. BGI-Shenzhen, Shenzhen, 518083, China.
E-mail addresses: liuya1@genomics.cn (Y. Liu), zidali@szu.edu.cn (Z. Li).
[1] Contributed equally.

https://doi.org/10.1016/j.bios.2022.114913
Received 25 July 2022; Received in revised form 9 November 2022; Accepted 11 November 2022
Available online 12 November 2022

clinical development. Transcriptome analysis provides a comprehensive picture of gene expression and can characterize the biological effects of the drugs in-depth. In addition to the drug effects on the target, transcriptome analysis can also examine off-target effects and thus predict the adverse effects in late-stage drug development, supporting early-stage decision-making (Verbist et al., 2015). Based on HTS tools, drug discovery experiments with transcriptional profiling have been implemented using gene chips (Lamb et al., 2006; Subramanian et al., 2017) or RNA sequencing (Ye et al., 2018). However, the throughput and cost efficiency of these methods still have room for improvement.

Finally, current drug discovery experiments are mostly performed on bulk samples, providing the response on the population average. Given the ubiquitous cellular heterogeneity, cells respond to drugs differently even among the same type, and the existence of a rare subtype may result in drug resistance and disease relapse. Therefore, analysis on the single-cell level is desirable (Wu et al., 2020).

A few works have been reported to address these technical challenges in drug screening. Microfluidics has been adopted to develop high throughput combinatorial screening using programmable microvalves (Eduati et al., 2018; Rane et al., 2015; Schuster et al., 2020; Li et al., 2022), microwells (Kulesa et al., 2018), micropillars (Li et al., 2018), or multilayered channels (Li et al., 2021). However, these methods used simple phenotypes such as proliferation rate as the readouts. Transcriptome analysis has been implemented to characterize cell responses to drug perturbations more comprehensively (Ye et al., 2018), and single-cell RNA sequencing (scRNA-seq) has been proposed to further tease out the heterogeneous response among the cell populations, provided that the perturbation information can be properly indexed into the sequencing results. To this end, barcoding strategies based on oligo transfection (Shin et al., 2019), single-nucleotide polymorphism (McFarland et al., 2020), and nuclear hashing (Srivatsan et al., 2020) have been developed to examine the transcriptomic response to perturbations on the single-cell level. Nevertheless, the operations of these techniques relied on microtiter plates as the reactors. Given the scale of combinatorial perturbation screening, both the workload and reagent consumption can be unbearable when used for such applications. An open microwell array chip with barcoded beads was developed to achieve single organoid culture and RNA sequencing (Wu et al., 2022), but this technique required spotting beads with the same barcodes in each microwell, making it difficult to scale up. Therefore, techniques that can perform single-cell transcriptomic analysis on combinatorial perturbations are yet to be developed.

Leveraging the advantage of droplet microfluidics in developing high throughput assays (Kulesa et al., 2018; Chung et al., 2019), here we report combinatorial perturbation sequencing (CP-seq) which can simultaneously perturb cells with drug combinations in a highly multiplexed fashion and perform single-cell transcriptomic analysis. CP-seq encapsulates cells and oligo-coded drugs in microdroplets, respectively, and performs droplet pairing in specially designed microwells, where two drug droplets randomly pair with one cell droplet, to complete the combinatorial perturbation, before the cells are subject to scRNA-seq. Since the drug barcodes are compatible with scRNA-seq workflow, the perturbation of individual cells can be recovered from the sequencing data. We first demonstrated the robust performance of the droplet operation, showing that 83% of the microwells were effectively utilized for droplet pairing and merging. We then validated CP-seq by first performing treatment of single drugs with known effects, showing the effectiveness of the experimental process. We further validated CP-seq by imposing combinatorial drug treatment, and the scRNA-seq results confirmed the efficacy. CP-seq can potentially perform drug treatment of up to a thousand combinations on a glass-slide-sized microfluidic chip, and the capability can be further scaled up by making larger chips. We envision that CP-seq would serve as a versatile tool for high throughput screening with comprehensive profiling on the single-cell level and greatly facilitate drug discovery.

2. Methods

2.1. Design and fabrication of microfluidic devices

Three microfluidic devices were used, including two droplet generators for cell and drug encapsulation, respectively, and one microwell array device for droplet pairing. Droplet generators adopted flow-focusing structures driven by negative pressure, and the channel heights were 90 and 40 μm throughout for cell and drug encapsulation, respectively. The microwell array device was composed of a layer with microwell arrays and a layer with a flow chamber. The depths of the microwells and the flow chamber were 70 μm and 220 μm, respectively, in the device for combinatorial treatment. In the device for single drug treatment, the depths of large and small microwell were 80 and 50 μm, respectively. Other dimensions are shown in Fig. S1. Device fabrication follows standard SU-8 photolithography and polydimethylsiloxane (PDMS) replica molding, as described in Supplementary Methods.

2.2. Cell and reagent preparation

The cell culture is described in the Supplementary Methods. Cell densities of 8,000 cells/μL were adopted for the generation of cell droplets. Reagent information is listed in Table S1. Four drugs were used in the experiment, namely doxorubicin hydrochloride (DOX), fluorouracil (5-FU), cyclophosphamide (CP), and paclitaxel (PTX). DOX and CP were dissolved in water of molecular biology grade, and 5-FU and PTX were dissolved in dimethyl sulfoxide (DMSO) following the supplier's suggestion. Three different concentrations of each drug were used, and the concentrations are listed in Table S2.

2.3. Design and preparation of the concanavalin A-based drug barcode (CADB) complex

The drug barcode consists of a PCR handle, a unique 10–base barcode, and a 21-base poly(A) tail. Full sequences are listed in Table S3. The oligonucleotides were synthesized and biotinylated by BGI Tech Solutions (Beijing). Upon arrival, the biotinylated oligonucleotides were diluted in nuclease-free water at a concentration of 100 nM. Biotinylated concanavalin A and streptavidin were dissolved in 50% glycerol at a concentration of 1.6 μM separately. To assemble the CADB complex, streptavidin was first mixed with biotinylated oligonucleotides and incubated for 10 min at room temperature, before biotinylated concanavalin A was added and incubated for 10 min at room temperature.

2.4. Droplet generation and manipulation

Droplets were generated by filling reservoirs with either oil or the aqueous phase and applying negative pressure at the outlet. Negative pressure was applied by pulling an air-filled syringe. The 87 μm cell droplets, 43 μm drug droplets, and 50 μm drug droplets were generated by pulling a 30 mL plastic syringe (302833, BD) from the initial position of 15 mL–20 mL, 15 mL–20 mL, and 17 mL–20 mL respectively. A cryovial (431386, Corning) was punched and connected between the syringe and the device outlet for droplet collection. The generated cell droplets were stored on ice, and the generated drug droplets were gently pooled for later use. After loading into the microwell array device, droplets were merged by treating the PDMS device with corona for 5 s using a handheld corona treater (BD-20AC, Electro-Technic Products, Chicago). Droplets were then retrieved into a centrifuge tube for incubation. After incubation, droplets were demulsified by slowly adding 1H,1H,2H,2H-perfluoro-1-octanol (PFO) into the oil. After washing, cells were resuspended in PBS solution containing 0.04% BSA.

2.5. Single-cell RNA sequencing (scRNA-seq) and analysis

The library preparation for scRNA-seq used the DNBelab C4 (MGI

Tech Co., Shenzhen) following the protocol as previously described (Liu et al., 2019). DNA double clean-up was performed to obtain both the cDNA and oligonucleotide product. Sequencing data were analyzed using STAR (Dobin et al., 2013), PISA (Shi et al., 2022), Seurat (Stuart et al., 2019), and "clusterProfiler" package (Wu et al., 2021). Details are discussed in the Supplementary Methods.

3. Results

3.1. Workflow of the CP-seq technology

To achieve multiplexity, CP-seq uses oligonucleotide (oligo) sequences to code the drug information and uses concanavalin A (ConA), which is a glycoprotein-binding protein applied in cell membrane labeling (Fang et al., 2021a), as the linker to tag the oligo barcodes to cell membranes, as shown in Fig. 1a. The oligo mainly consists of a PCR handle, a unique 10-base barcode to store drug information, and a 21-base poly(A) tail for downstream capturing. By conjugating ConA with oligo, the complex of ConA-based drug barcode (CADB) is created. Each drug solution is mixed with a designated CADB complex that encodes the drug condition, including the drug molecule and dose, and the mix is encapsulated into droplets, as shown in Fig. 1b. The continuous phase used fluorinated oil supplemented with a surfactant to prevent premature coalescence. All drug droplets are then pooled, resulting in a drug library in the form of droplets. Meanwhile, cells are encapsulated into droplets that are larger than the drug droplets. Since CP-seq does not require single-cell encapsulation, an additional step of droplet sorting is not necessary.

The combinatorial drug treatment is performed in a microfluidic device consisting of an upper layer of microwell array facing down and a lower layer of flow chamber (Fig. 1c; Fig. S1; Video S1). Each microwell unit consists of two interconnected microwells, with a diameter of 90 and 50 μm, respectively. The depth of the microwells is 70 μm. A glass slide-sized chip houses roughly 26,800 microwell units. Cell droplets, with diameters of 87 μm, are first loaded into the flow chamber. Since water is much lighter than the continuous phase of oil (~1.6 g/mL), the droplets float into the microwell and occupy the large half of each microwell unit, leaving out the small half. Drug droplets, with smaller diameters of 43 μm, are then loaded into the flow chamber and float into the small half of each microwell unit. Since the microwells are relatively deep, with proper quality control on the droplet dimension, each microwell captures precisely two drug droplets. The cell droplet and the two drug droplets are merged using corona treatment. The droplets are then retrieved and incubated to complete the combinatorial drug treatment before the cells are subject to single-cell RNA sequencing (scRNA-seq). Sequencing beads capture both the mRNA and drug barcode oligos by the functionalized poly(T) on the bead surface, as shown in Fig. 1d and Fig. S2, and consequently, both the transcriptome and the two drug barcodes can be recovered from the sequencing data.

Supplementary data related to this article can be found at https://doi.org/10.1016/j.bios.2022.114913.

3.2. Performance of the microfluidic manipulation of droplets

The robust performance of droplet manipulation is the foundation of the CP-seq technology. Therefore, we first sought to characterize and optimize the operation parameters related to droplet manipulation. Uniform droplets were generated using flow-focusing devices driven by negative pressure at the outlet, and the resultant cell and drug droplets were 86.8 ± 3.7 μm (n = 498) and 42.3 ± 1.5 μm (n = 480) in diameters,

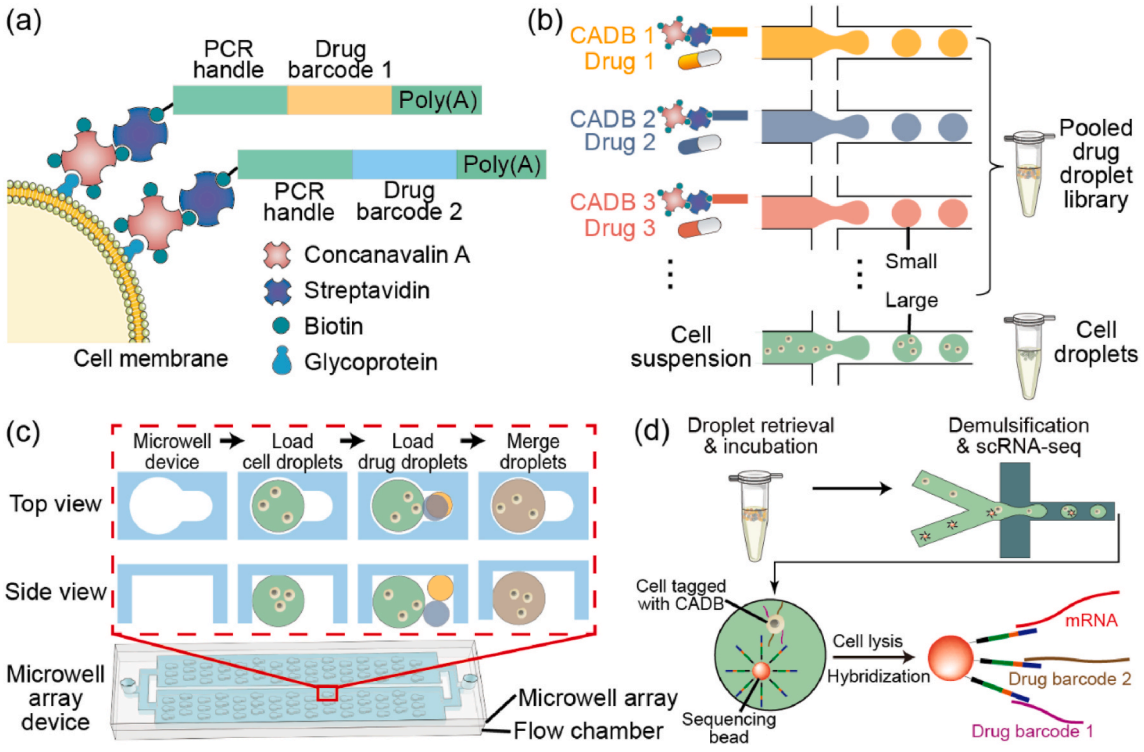

Fig. 1. Overview of the combinatorial perturbation sequencing technology. (a) Schematic showing the principle of cell tagging with the drug barcode. Concanavalin A, which is conjugated with a designated oligonucleotide sequence, binds to the cell membrane and thus tags the cell. (b) Barcoded drug droplets and cell droplets with differential diameters are generated using microfluidics. Drugs are pre-mixed with the concanavalin A-based drug barcode (CADB). (c) Cell droplets are loaded into the microwell array device and occupy the large microwells, before drug droplets are loaded and occupy the small microwells. Each small microwell randomly captures two drug droplets. Droplets in each microwell unit are merged via corona treatment, resulting in combinatorial drug treatment and CADB tagging on cells. (d) Droplets are then incubated and demulsified to collect cells for single-cell RNA sequencing (scRNA-seq). The sequencing bead simultaneously captures mRNA and drug barcodes through the poly(T) tail.

respectively, with variations less than 5% (Fig. 2a&b; Fig. S1). Using a cell density of 8,000 cells/μL, 97.9% of the cell droplets contained one or more cells, with 67% containing two to four cells, accounting 1,997 droplets.

The droplet trapping and pairing on the microwell array device also showed robust performance. After cell droplet loading, more than 99% of the microwells were occupied by a cell droplet (Fig. 2d). After drug droplet loading, more than 92% of the microwells captured two drug droplets (Fig. 2e). The microwell array device was then subject to a brief corona treatment, resulting in interface destabilization and subsequent droplet merging. By slightly tilting the device and ensuring that all three droplets were in contact, more than 90% of the microwells were merged after the corona treatment (Fig. 2f). By flipping over the device, nearly all the droplets floated out of the microwells and could be collected at the outlet (Video S1). In the process of droplet pairing, the size of the drug droplets was an important parameter. For example, when drug droplets had a diameter of 50 μm instead of 43 μm, only 20.4% of microwells captured two droplets, and 77.7% of microwells captured one droplet, calculated on 1,078 microwells (Fig. 2g).

Though cell culture in droplets has been well studied (Sart et al., 2022), corona treatment is a less standard operation. Corona treatment generates an instant but strong electric potential, which may impose a disturbance on the gene expression of the cells. Therefore, we specifically investigated the effect on cells of the dose of corona treatment in our experiment setting, which was 5 s. We performed scRNA-seq on MCF-7 cells immediately and 2 h after 5 s' corona treatment and compared them with those not treated with a corona at all. After dimensionality reduction using Uniform Manifold Approximation and Projection (UMAP), the transcriptome data were highly overlapping among the three groups, suggesting that the brief treatment with corona had a negligible effect on cells (Fig. 2h).

3.3. Validation of the CP-seq using single-drug treatment

We then sought to validate CP-seq's performance in profiling single-cell transcriptomes on drug perturbations. The gene expression after the treatment of a specific chemotherapy drug has been well studied, and it offers a good reference for comparison. Therefore, we first performed single-drug treatment using the CP-seq technology to validate the processes involving scRNA-seq and drug demultiplexing.

The microwell array device in CP-seq was adapted by reducing the depth of the small microwell to allow the trapping of a single drug droplet (Fig. 3a). Consequently, more than 97% of the microwell units captured a cell droplet and a single drug droplet (Fig. 3b). Using this microwell array device, we first characterized the performance of CADB binding and recovering using qPCR. We designed oligo with poly(A) tail, the accompanying reverse transcription primer, and PCR amplification primers (Table S4). The oligo was conjugated to ConA, and the resultant CADB complex was used as the "drug" to treat and tag cells following the CP-seq experimental protocol. After "drug" treatment, instead of performing scRNA-seq, reverse transcription and qPCR were performed on the cell lysis to quantify the oligo. The oligo was successfully detected,

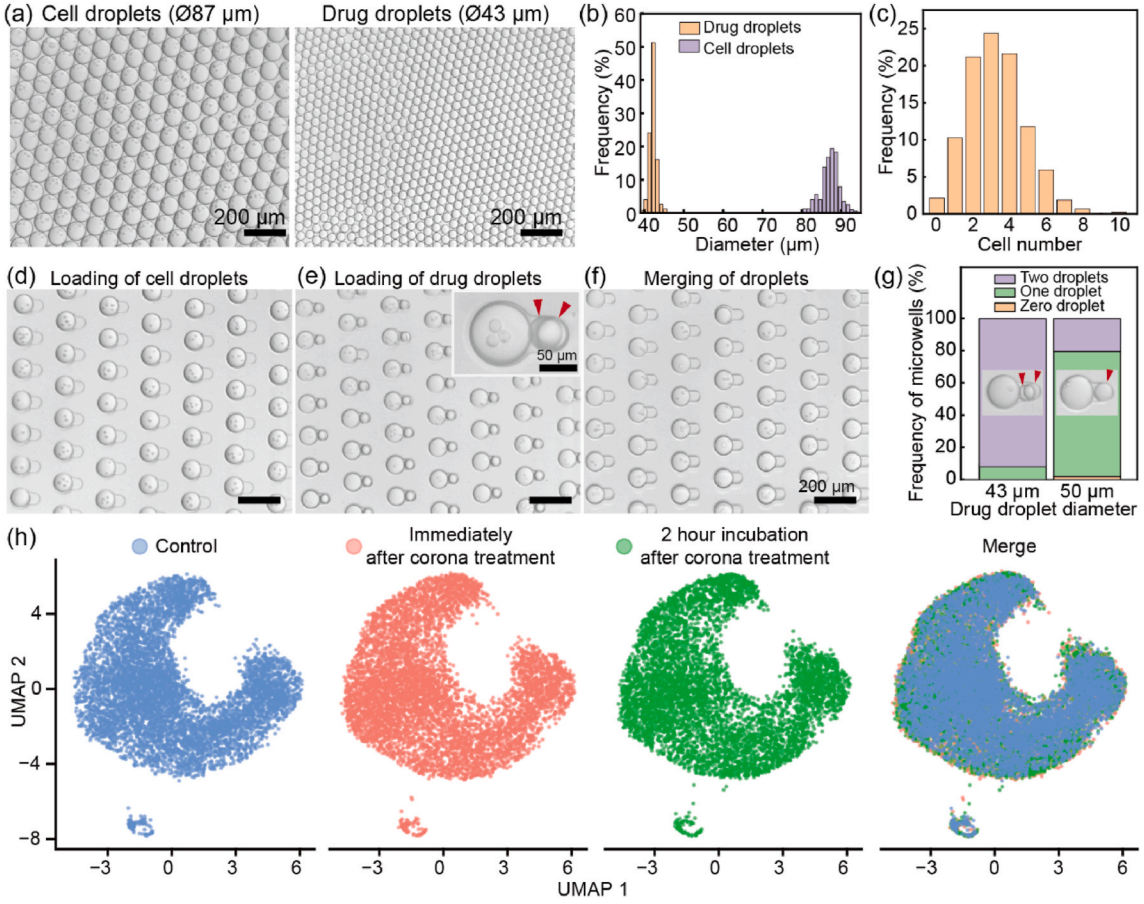

Fig. 2. Performance of the droplet manipulation platform. (a) Micrographs of the generated cell droplets and drug droplets. (b) Diameter distribution of the cell droplets (n = 498) and drug droplets (n = 480). (c) Distribution of the cell numbers in each cell droplet (n = 1,997). (d–f) Micrographs showing the process of cell droplet loading, drug droplet loading, and droplet merging, with microwell utilization rates being 99.9 ± 0.1%, 91.6 ± 2.6%, and 90.0 ± 1.0%, respectively. Simultaneous capturing of two drug droplets can be identified under a bright-field microscope, as indicated by red arrows. Data represent mean ± standard deviation with n = 3, sampling 4,050 microwells in each replicate. (g) Frequency of microwells occupied by different numbers of droplets when using droplets of different diameters, calculated on 1,078 microwells. (h) UMAP plot of the scRNA-seq data showing the effect of the corona treatment on cells.

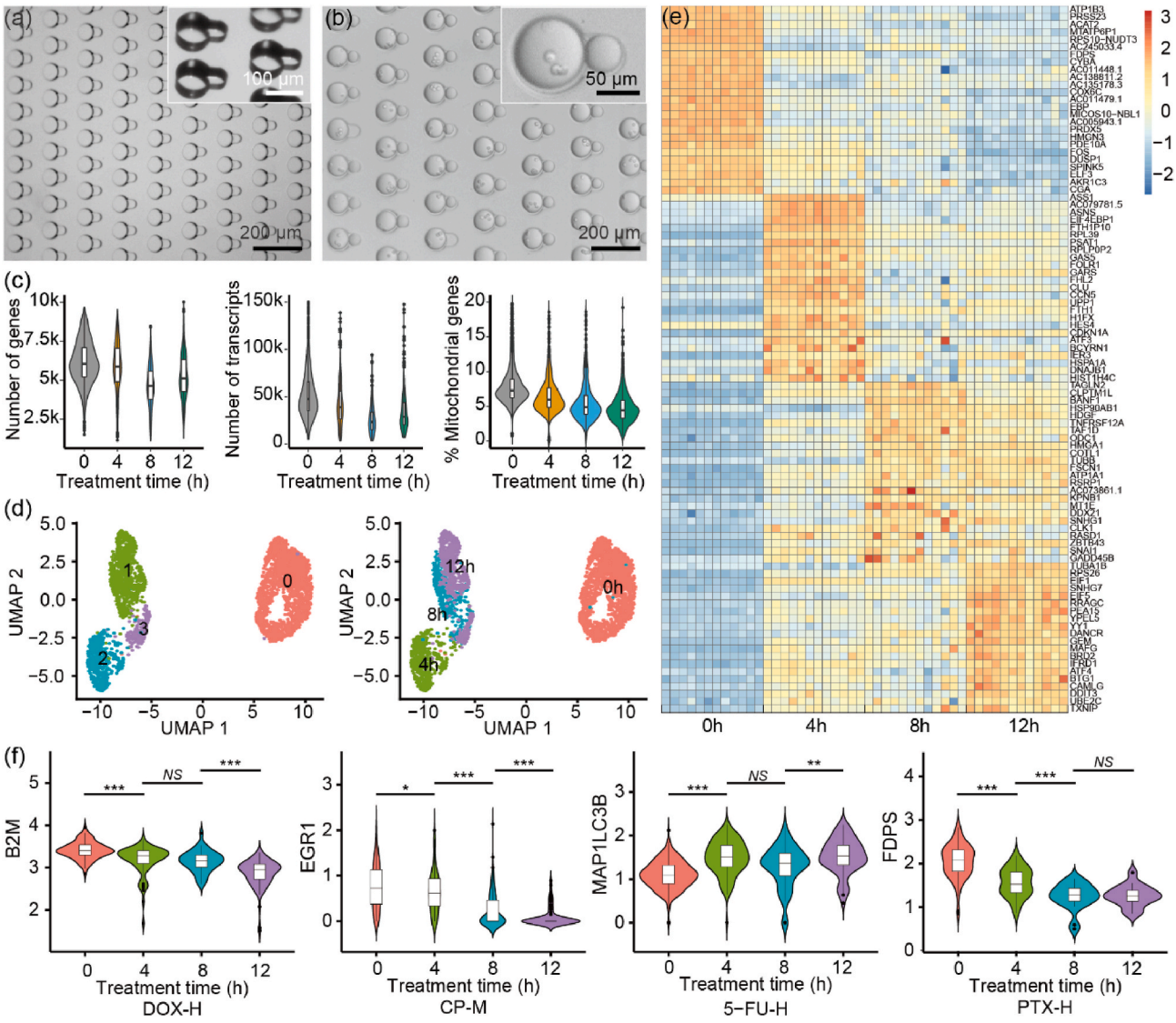

Fig. 3. Validation of the CP-seq using single drug treatment. (a) Micrograph showing the microwell device used to capture single drug droplets. Microwells with differential depths were designed. Inset: close-up view of the microwell unit under a stereomicroscope. (b) Micrograph showing the capturing of cell droplets and single drug droplets. (c) Quality assessment of the scRNA-seq results under drug treatment of 0, 4, 8, and 12 h. (d) Scatter plot of UMAP analysis showing the cell clustering. (e) Heatmap showing the gene expression at different time points. Each column represents a drug treatment condition at the corresponding time point. (f) Temporal gene expression of representative genes. *, $p < 0.05$. **, $p < 0.01$. ***, $p < 0.001$. *N.S.*, not significant.

and the qPCR results showed that on average about 18,600 oligo molecules were recovered from each cell, consistent with reported works (Fig. S3). (Fang et al., 2021b) These results suggested that the droplet manipulation was fully operational and that the CADB-based cell labeling and barcoding were successful.

We then sought to perform the single drug treatment on cells. We chose breast cancer cell (MCF-7) and four commonly used chemotherapy drugs, namely doxorubicin (DOX), paclitaxel (PTX), 5-fluorouracil (5-FU), and cyclophosphamide (CP), for the study. Three doses for each drug, suffixed with L (low), M (medium), and H (high), were incorporated in the experiments, resulting in 13 groups including the vehicle control (Table S2). In addition, we sought to profile the single-cell transcriptome with different incubation times to obtain the temporal development of gene expression. To obtain a suitable timeframe for drug treatment, we first performed cell viability assays since live cells were necessary for scRNA-seq. The results showed the viability had a sharp drop upon 16 h of treatment (Fig. S4). Therefore, we chose 4, 8, and 12 h as the incubation times. To investigate the effect of in-droplet cell culture on cell viability, we generated droplets with cells and plain medium, incubated cells for different durations, and retrieved cells from the droplets to perform viability staining. The results showed that cell viability was above 95% throughout 24 h of incubation, suggesting that in-droplet cell culture does not affect cell viability (Fig. S5). In addition, we characterized the inter-droplet diffusion of drugs and CADB using different types of tracing reagents. The results showed the diffusion of water-dissolved drugs, DMSO-dissolved drugs, and CADB were all negligible (Fig. S6).

We performed the CP-seq with the 13 treatment groups, and each drug condition was designated with a CADB barcode shown in Table S3. After drug treatment, the cells were incubated for 0, 4, 8, and 12 h as separate experiments, and the cells then went through scRNA-seq. The scRNA-seq results showed good quality. The number of genes detected in each cell on average ranged from 4,000 to 6,000, the numbers of transcripts were more than 15,000, and the percentages of mitochondrial genes were around 5% in experiments of different incubation times (Fig. 3c). After alignment and error correction, we detected 3,243 cells with corresponding drug treatment recovered. We then performed dimensionality reduction using uniform manifold approximation and

projection (UMAP) to visualize the transcriptomes of cells incubated for different times. As shown in Fig. 3d, the drug-treated cells showed distinct transcriptomes compared to the control group (0 h). Among drug-treated cells, those of the same incubation time were near each other, and the clustering results reasonably agreed with the experimental conditions of incubation time. We further visualized the temporal development of the average expression of the top 100 genes using a heatmap (Fig. 3e). The heatmap showed the gradual change over time of the gene expression profiles. We then examined a few genes with known consequences upon drug treatments, and the results agreed with the established drug knowledge. For example, as shown in Fig. 3f, the down-regulation of the B2M and EGR1 gene due to DOX and CP treatment were both observed (Beckwitt, 2018), and the up-regulation of the MAP1LC3B gene, which was responsive to DNA damage, due to 5-FU treatment was also observed (Park et al., 2020). We also observed gene regulations that were previously not reported, such as the down-regulation of the FDPS gene upon PTX treatment, which might hold biological insights and could be further investigated.

3.4. Validation of the CP-seq using combinatorial drug treatment

We then performed the complete process of the CP-seq for further validation. We used the above-mentioned 12 drug conditions (four drugs by three different doses) and a blank control for the experiments, and the incubation time was shortened to 1 h, given the low viability of cells on combinatorial drug treatment (Fig. S7). We additionally profiled the transcriptomes of cells immediately after drug treatment but without incubation for comparison.

We first sought to examine the drug barcoding performance. The number of combinations of two among the 13 drug conditions is 78; therefore, we expected to recover 78 barcode combinations from the sequencing data. In the no-incubation group, we recovered 71 combinations, as visualized in the chord diagram in Fig. 4a. Seven combinations were missing, likely because of the data filtering in postprocessing which discarded transcriptomes of low quality. In the incubation group, we recovered 47 treatment combinations, which were fewer than that in the no-incubation group, presumably because of the cell death induced by the combinatorial treatment. We then compared the gene expression patterns in these two experimental groups using Gene Ontology (GO) enrichment analysis. Since the four drugs used in the experiments were all related to DNA damage and cell apoptosis and had a similar effect on cells, we pooled the experiment groups for the analysis. In particular, we adopted cellular component ontology (CCO) terms to analyze the differences in cellular components between these two experiment groups. The results showed that the GO-CCO terms enriched in the group without incubation were mainly related to chromosomes in the nucleus, the genes of which perform functions such as mitosis (Fig. 4b). In contrast, the GO terms enriched in the group with 1-h incubation were mainly ribosomal and mitochondrial components, likely indicating high cell stress. We then sought to examine the transcriptomic impact of combinatorial drug treatment compared to single drug treatment. Since combinatorial drug therapy generally induces stronger responses from cells, the validity of CP-seq could be demonstrated if the gene expression under combinatorial drug treatment showed more drastic alteration compared to single drug treatment. For ease of analysis, we pooled the data of each experimental group and analyzed the differential gene expression. As shown in Fig. 4c, the analysis visualized the up-regulation of tens of genes and the down-regulation of about 500 genes, which

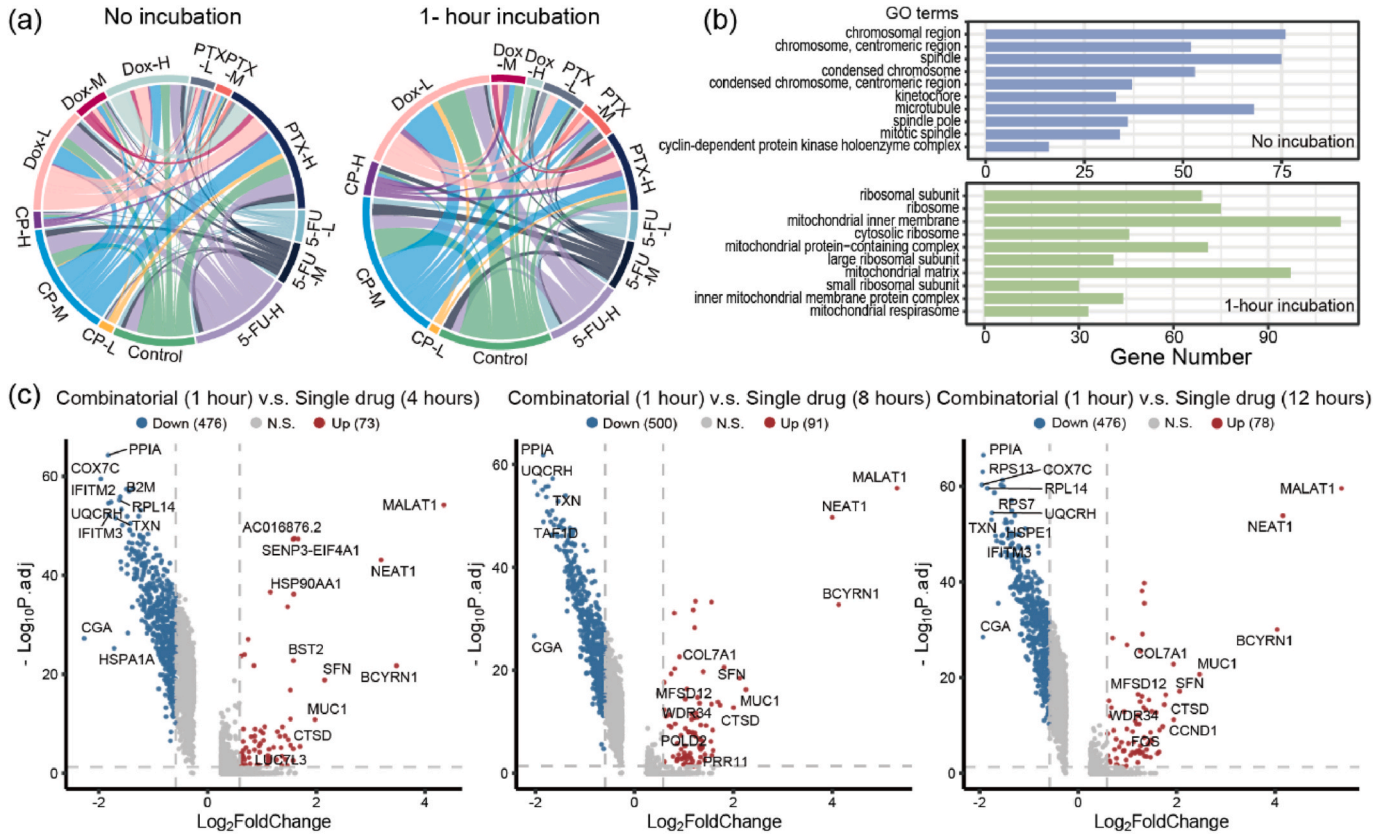

Fig. 4. Validation of the CP-seq using combinatorial drug treatment. (a) Chord diagrams showing the drug combinations recovered from the sequencing data in groups with no incubation and 1-h incubation. (b) Histogram showing the top ten Gene Ontology (GO) terms of cell component assigned to the above two transcriptomes. Results were ranked based on the adjusted p-value. (c) Volcano plots showing the differential gene expression of cells with combinatorial drug treatment for an hour compared to single drug treatment for 4 h, 8 h, and 12 h. Genes that have an adjusted *p*-value smaller than 0.05 and an absolute value of fold change larger than 1.5 were considered significant.

demonstrated the capability of the CP-seq in profiling gene expression under combinatorial drug treatment. We further analyzed the differential expression of a few representative genes relative to the single drug treatment. For example, MALAT1, which is related to cell stress (Zhang et al., 2012), was indeed up-regulated, and NEAT1, which was reported to participate in the cross-regulation among apoptosis, pyroptosis, autophagy, and ferroptosis (Zhang et al., 2022), was also up-regulated. In addition, B2M, which is a housekeeping gene for the maintenance of basic cell function (Kılıç et al., 2014), was downregulated. The agreement between the sequencing results under combinatorial perturbation and the known knowledge suggested the validity of CP-seq.

4. Conclusions and discussion

In this work, we developed a technology, named combinatorial perturbation sequencing (CP-seq), to obtain single-cell transcriptomes upon combinatorial drug treatments using droplet microfluidics. In the experiments with 13 single-drug conditions, CP-seq recovered 71 drug combinations out of the 78 possible combinations, showing the potential of CP-seq in finding new efficacious drug combinations.

Since a glass slide-sized chip houses roughly 26,800 microwell units and each microwell holds 3 cells on average, a chip can accommodate 1,300 drug combinations in principle, assuming that a sample size of 20 microwell units (~60 cells in total) is enough for the downstream analysis of each drug treatment. In addition to combinations of two drugs, CP-seq holds the versatility of being adapted to test combinations of multiple drugs by incorporating additional small microwells in each microwell unit.

Nevertheless, though the throughput of CP-seq can be easily scaled up by designing larger devices of microwell arrays, the generation of the drug droplet library can be labor-intensive if the drug library contains thousands of drugs, since the droplets of each drug are currently generated separately. A strategy to resolve this challenge is to adopt techniques that generate droplets with high automation. For example, the commercial instruments of microarray spotters can be utilized to generate a high-volume droplet library, as demonstrated in Fig. S8 and by reported works (Zhang et al., 2021). With such droplet generation techniques, drug droplet libraries of high volume can be prepared with minimal human intervention. In addition, by integrating the cell droplet generation module and the droplet pairing module and forming a fully automated system with minimal human intervention, the usability of CP-seq can be further improved. Finally, though CP-seq was able to recover a significant number of cells after the single drug perturbation, the cell recovery rate after combinatorial perturbation was suboptimal. In addition, the cross-contamination of drug droplets induced by inter-droplet diffusion, especially for DMSO-dissolved drugs, may cause issue in some applications. Future work could be devoted to the optimization of reagent operation and in-depth analysis of the perturbed transcriptomes, further enabling the practical applications of this technique.

CRediT authorship contribution statement

Run Xie: Methodology, Validation, Formal analysis, Investigation, Writing – original draft. **Yang Liu:** Conceptualization, Methodology, Validation, Formal analysis, Investigation, Writing – original draft. **Shiyu Wang:** Conceptualization, Methodology, Formal analysis. **Xuyang Shi:** Formal analysis. **Zhantao Zhao:** Validation. **Longqi Liu:** Conceptualization, Project administration. **Ya Liu:** Conceptualization, Methodology, Supervision. **Zida Li:** Conceptualization, Methodology, Writing – review & editing, Supervision.

Declaration of competing interest

The authors declare that they have no known competing financial interests or personal relationships that could have appeared to influence the work reported in this paper.

Data availability

Data will be made available on request.

Acknowledgments

The authors thank Xiaoxiang Hu and Prof. Yujuan Chai for sharing equipment. This work was supported by the National Key Research and Development Program of China (2021YFF1200500), Guangdong Basic and Applied Basic Research Foundation (2021A1515110459), Shenzhen Overseas Talent Program, and Shenzhen University Faculty Startup Grant.

Appendix A. Supplementary data

Supplementary data to this article can be found online at https://doi.org/10.1016/j.bios.2022.114913.

References

Al-Lazikani, B., Banerji, U., Workman, P., 2012. Combinatorial drug therapy for cancer in the post-genomic era. Nat. Biotechnol. 30 (7), 679–692.
Beckwitt, C.H., 2018. In Breast Cancer Metastatic Dormancy and Emergence, a Role for Adjuvant Statin Therapy.
Bhutani, P., Joshi, G., Raja, N., Bachhav, N., Rajanna, P.K., Bhutani, H., Paul, A.T., Kumar, R., 2021. U.S. FDA approved drugs from 2015–June 2020: a perspective. J. Med. Chem. 64 (5), 2339–2381.
Brown, R., Curry, E., Magnani, L., Wilhelm-Benartzi, C.S., Borley, J., 2014. Poised epigenetic states and acquired drug resistance in cancer. Nat. Rev. Cancer 14 (11), 747–753.
Chung, M.T., Kurabayashi, K., Cai, D., 2019. Single-cell RT-LAMP mRNA detection by integrated droplet sorting and merging. Lab Chip 19 (14), 2425–2434.
Dobin, A., Davis, C.A., Schlesinger, F., Drenkow, J., Zaleski, C., Jha, S., Batut, P., Chaisson, M., Gingeras, T.R., 2013. STAR: ultrafast universal RNA-seq aligner. Bioinformatics 29 (1), 15–21.
Eduati, F., Utharala, R., Madhavan, D., Neumann, U.P., Longerich, T., Cramer, T., Saez-Rodriguez, J., Merten, C.A., 2018. A microfluidics platform for combinatorial drug screening on cancer biopsies. Nat. Commun. 9 (1), 2434.
Fang, L., Li, G., Sun, Z., Zhu, Q., Cui, H., Li, Y., Zhang, J., Liang, W., Wei, W., Hu, Y., Chen, W., 2021a. CASB: a concanavalin A-based sample barcoding strategy for single-cell sequencing. Mol. Syst. Biol. 17 (4), e10060.
Fang, L., Li, G., Sun, Z., Zhu, Q., Cui, H., Li, Y., Zhang, J., Liang, W., Wei, W., Hu, Y., Chen, W., 2021b. CASB: a concanavalin A-based sample barcoding strategy for single-cell sequencing. Mol. Syst. Biol. 17 (4).
Jaaks, P., Coker, E.A., Vis, D.J., Edwards, O., Carpenter, E.F., Leto, S.M., Dwane, L., Sassi, F., Lightfoot, H., Barthorpe, S., van der Meer, D., Yang, W., Beck, A., Mironenko, T., Hall, C., Hall, J., Mali, I., Richardson, L., Tolley, C., Morris, J., Thomas, F., Lleshi, E., Aben, N., Benes, C.H., Bertotti, A., Trusolino, L., Wessels, L., Garnett, M.J., 2022. Effective drug combinations in breast, colon and pancreatic cancer cells. Nature 603 (7899), 166–173.
Kılıç, Y., Çelebiler, A.Ç., Sakızlı, M., 2014. Selecting housekeeping genes as references for the normalization of quantitative PCR data in breast cancer. Clin. Transl. Oncol. 16 (2), 184–190.
Kulesa, A., Kehe, J., Hurtado, J.E., Tawde, P., Blainey, P.C., 2018. Combinatorial drug discovery in nanoliter droplets. Proc. Natl. Acad. Sci. U. S. A. 115 (26), 6685–6690.
Lamb, J., Crawford, E.D., Peck, D., Modell, J.W., Blat, I.C., Wrobel, M.J., Lerner, J., Brunet, J.-P., Subramanian, A., Ross, K.N., Reich, M., Hieronymus, H., Wei, G., Armstrong, S.A., Haggarty, S.J., Clemons, P.A., Wei, R., Carr, S.A., Lander, E.S., Golub, T.R., 2006. The connectivity map: using gene-expression signatures to connect small molecules, genes, and disease. Science 313 (5795), 1929–1935.
León-Buitimea, A., Garza-Cárdenas, C.R., Garza-Cervantes, J.A., Lerma-Escalera, J.A., Morones-Ramírez, J.R., 2020. The demand for new antibiotics: antimicrobial peptides, nanoparticles, and combinatorial therapies as future strategies in antibacterial agent design. Front. Microbiol. 11.
Li, J., Tan, W., Xiao, W., Carney, R.P., Men, Y., Li, Y., Quon, G., Ajena, Y., Lam, K.S., Pan, T., 2018. A plug-and-play, drug-on-pillar platform for combination drug screening implemented by microfluidic adaptive printing. Anal. Chem. 90 (23), 13969–13977.
Li, L., Chen, Y., Wang, H., An, G., Wu, H., Huang, W., 2021. A high-throughput, open-space and reusable microfluidic chip for combinational drug screening on tumor spheroids. Lab Chip 21, 3924–3932.
Li, H., Zhang, P., Hsieh, K., Wang, T.-H., 2022. Combinatorial nanodroplet platform for screening antibiotic combinations. Lab Chip 22, 621–631.
Liu, C., Wu, T., Fan, F., Liu, Y., Wu, L., Junkin, M., Wang, Z., Yu, Y., Wang, W., Wei, W., Yuan, Y., Wang, M., Cheng, M., Wei, X., Xu, J., Shi, Q., Liu, S., Chen, A., Wang, O., Ni, M., Zhang, W., Shang, Z., Lai, Y., Guo, P., Ward, C., Volpe, G., Wang, L., Zheng, H., Liu, Y., Peters, B.A., Beecher, J., Zhang, Y., Esteban, M.A., Hou, Y., Xu, X.,

Chen, I.-J., Liu, L., 2019. A portable and cost-effective microfluidic system for massively parallel single-cell transcriptome profiling. bioRxiv, 818450.
McFarland, J.M., Paolella, B.R., Warren, A., Geiger-Schuller, K., Shibue, T., Rothberg, M., Kuksenko, O., Colgan, W.N., Jones, A., Chambers, E., Dionne, D., Bender, S., Wolpin, B.M., Ghandi, M., Tirosh, I., Rozenblatt-Rosen, O., Roth, J.A., Golub, T.R., Regev, A., Aguirre, A.J., Vazquez, F., Tsherniak, A., 2020. Multiplexed single-cell transcriptional response profiling to define cancer vulnerabilities and therapeutic mechanism of action. Nat. Commun. 11 (1), 4296.
Park, S.R., Namkoong, S., Friesen, L., Cho, C.S., Zhang, Z.Z., Chen, Y.C., Yoon, E., Kim, C. H., Kwak, H., Kang, H.M., Lee, J.H., 2020. Single-cell transcriptome analysis of colon cancer cell response to 5-fluorouracil-induced DNA damage. Cell Rep. 32 (8), 108077.
Rane, T.D., Zec, H.C., Wang, T.-H., 2015. A barcode-free combinatorial screening platform for matrix metalloproteinase screening. Anal. Chem. 87 (3), 1950–1956.
Sart, S., Ronteix, G., Jain, S., Amselem, G., Baroud, C.N., 2022. Cell culture in microfluidic droplets. Chem. Rev.
Schuster, B., Junkin, M., Kashaf, S.S., Romero-Calvo, I., Kirby, K., Matthews, J., Weber, C.R., Rzhetsky, A., White, K.P., Tay, S., 2020. Automated microfluidic platform for dynamic and combinatorial drug screening of tumor organoids. Nat. Commun. 11 (1), 5271.
Shi, Q., Liu, S., Kristiansen, K., Liu, L., 2022. The FASTQ+ format and PISA. Bioinformatics 38 (19), 4639–4642.
Shin, D., Lee, W., Lee Ji, H., Bang, D., 2019. Multiplexed single-cell RNA-seq via transient barcoding for simultaneous expression profiling of various drug perturbations. Sci. Adv. 5 (5), eaav2249.
Srivatsan, S.R., McFaline-Figueroa, J.L., Ramani, V., Saunders, L., Cao, J., Packer, J., Pliner, H.A., Jackson, D.L., Daza, R.M., Christiansen, L., Zhang, F., Steemers, F., Shendure, J., Trapnell, C., 2020. Massively multiplex chemical transcriptomics at single-cell resolution. Science 367 (6473), 45.
Stuart, T., Butler, A., Hoffman, P., Hafemeister, C., Papalexi, E., Mauck 3rd, W.M., Hao, Y., Stoeckius, M., Smibert, P., Satija, R., 2019. Comprehensive integration of single-cell data. Cell 177 (7), 1888–1902 e21.
Subramanian, A., Narayan, R., Corsello, S.M., Peck, D.D., Natoli, T.E., Lu, X., 2017. A next generation connectivity map: L1000 platform and the first 1,000,000 profiles. Cell 171 (6), 1437–1452 e17.
Verbist, B., Klambauer, G., Vervoort, L., Talloen, W., Shkedy, Z., Thas, O., Bender, A., Göhlmann, H.W.H., Hochreiter, S., 2015. Using transcriptomics to guide lead optimization in drug discovery projects: lessons learned from the QSTAR project. Drug Discov. Today 20 (5), 505–513.
Wu, Z., Lawrence, P.J., Ma, A., Zhu, J., Xu, D., Ma, Q., 2020. Single-cell techniques and deep learning in predicting drug response. Trends Pharmacol. Sci. 41 (12), 1050–1065.
Wu, T., Hu, E., Xu, S., Chen, M., Guo, P., Dai, Z., Feng, T., Zhou, L., Tang, W., Zhan, L., Fu, X., Liu, S., Bo, X., Yu, G., 2021. clusterProfiler 4.0: a universal enrichment tool for interpreting omics data. Innovation 2 (3), 100141.
Wu, Y., Li, K., Li, Y., Sun, T., Liu, C., Dong, C., Zhao, T., Tang, D., Chen, X., Chen, X., Liu, P., 2022. Grouped-seq for integrated phenotypic and transcriptomic screening of patient-derived tumor organoids. Nucleic Acids Res. 50 (5), e28 e28.
Ye, C., Ho, D.J., Neri, M., Yang, C., Kulkarni, T., Randhawa, R., Henault, M., Mostacci, N., Farmer, P., Renner, S., Ihry, R., Mansur, L., Keller, C.G., McAllister, G., Hild, M., Jenkins, J., Kaykas, A., 2018. DRUG-seq for miniaturized high-throughput transcriptome profiling in drug discovery. Nat. Commun. 9 (1), 4307.
Zeng, W., Guo, L., Xu, S., Chen, J., Zhou, J., 2020. High-throughput screening technology in industrial biotechnology. Trends Biotechnol. 38 (8), 888–906.
Zhang, B., Arun, G., Mao, Yuntao S., Lazar, Z., Hung, G., Bhattacharjee, G., Xiao, X., Booth, Carmen J., Wu, J., Zhang, C., Spector, David L., 2012. The lncRNA Malat1 is dispensable for mouse development but its transcription plays a cis-regulatory role in the adult. Cell Rep. 2 (1), 111–123.
Zhang, J.Q., Siltanen, C.A., Dolatmoradi, A., Sun, C., Chang, K.-C., Cole, R.H., Gartner, Z. J., Abate, A.R., 2021. High diversity droplet microfluidic libraries generated with a commercial liquid spotter. Sci. Rep. 11 (1), 4351.
Zhang, Y., Luo, M., Cui, X., O'Connell, D., Yang, Y., 2022. Long noncoding RNA NEAT1 promotes ferroptosis by modulating the miR-362-3p/MIOX axis as a ceRNA. Cell Death Differ. 29 (9), 1850–1863.